Supplemental Figures

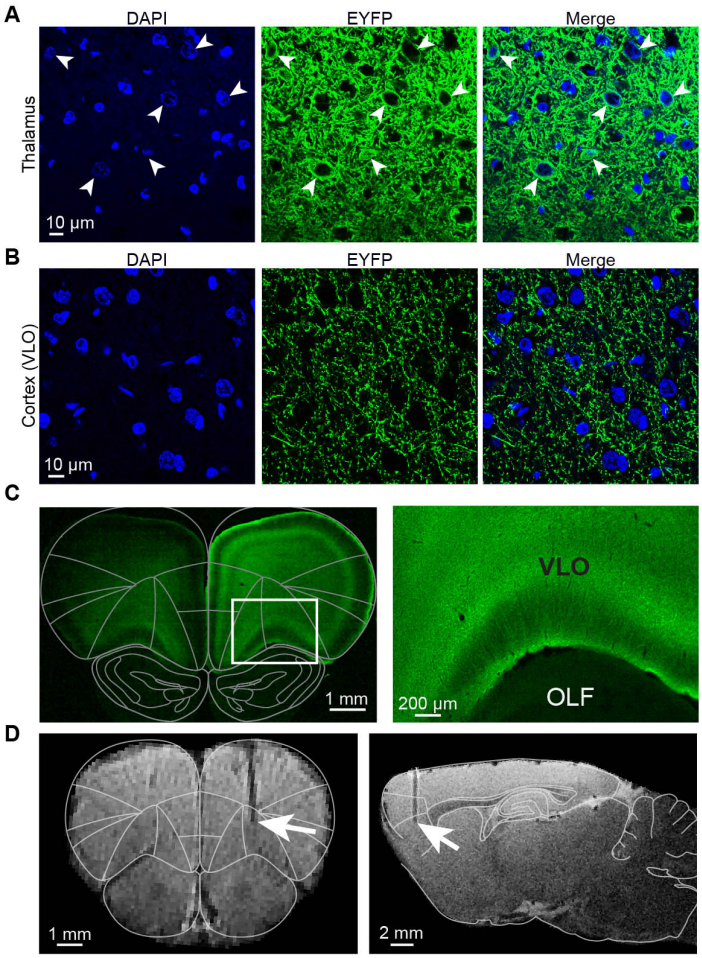

Figure S1. Stimulation was genetically and spatially targeted to thalamocortical projections in the ventrolateral subdivision of orbitofrontal cortex (VLO); Related to Figure 1. (*A*) Confocal imaging at the site of injection confirms ChR2-EYFP is expressed in cell bodies of thalamic neurons (white arrowheads). 29% of cells identified within the bulk injection area were ChR2-EYFP-positive (N=2 animals, 343 cells). (*B,C*) Confocal (B) and fluorescence (C) imaging in VLO confirms the presence of ChR2-EYFP-positive neuronal processes. ChR2-EYFP-positive cell bodies are not observed, verifying that stimulation was restricted to thalamocortical projections. OLF: olfactory bulb. Note that a secondary antibody, which emits in the red channel, was used to amplify the endogenous EYFP signal. This signal was mapped to the green channel for consistency with standard visualizations of EYFP. (*D*) Representative T2-weighted MRI scans used to confirm stimulation location in cortex. Arrows mark the location of light delivery at the fiber optic implant tip (left, coronal; right, sagittal).

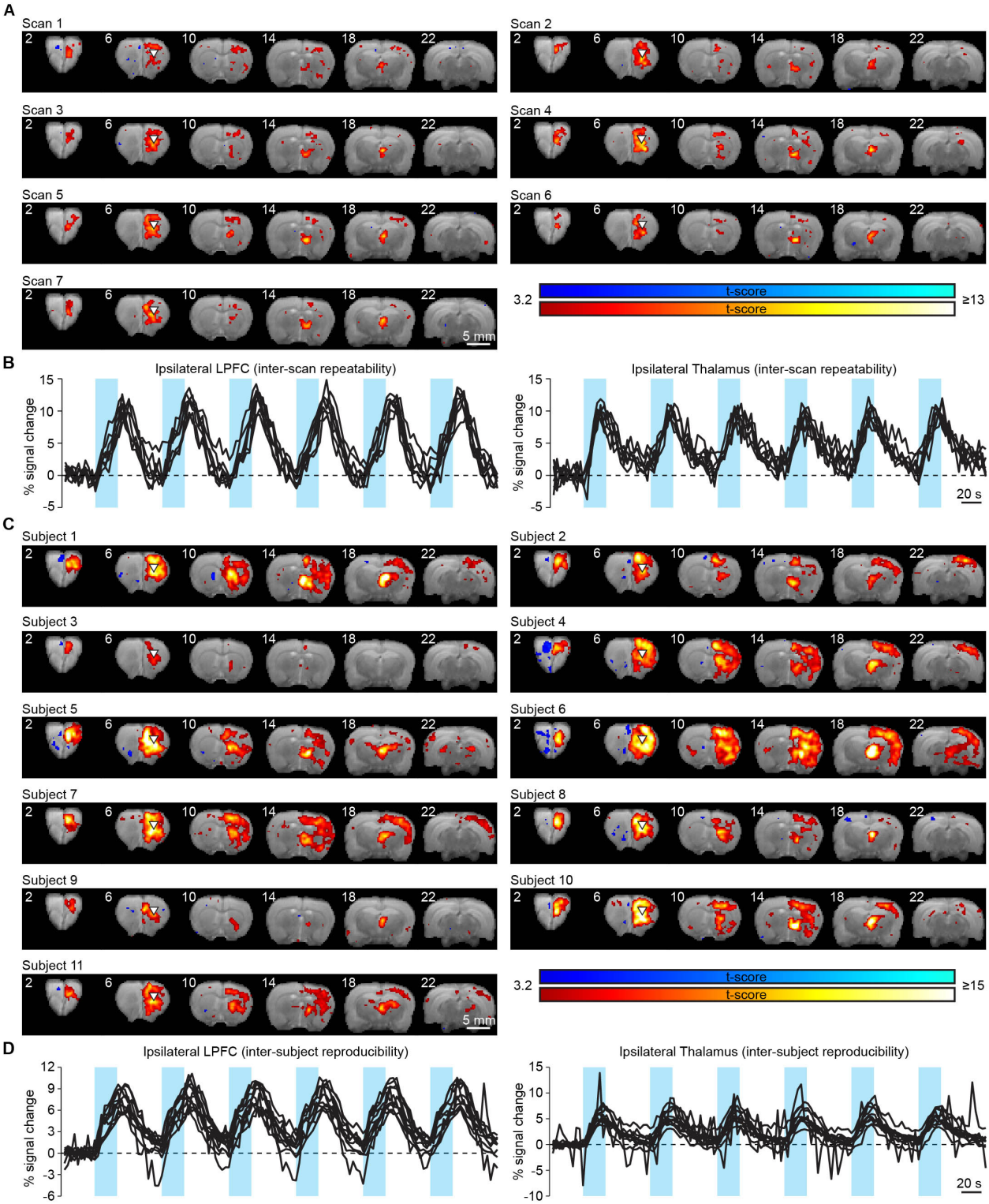

Figure S2. fMRI activations driven by thalamocortical stimulation were highly consistent across scans and subjects; Related to Figure 1. (*A*) Single-scan activation maps in response to 40 Hz thalamocortical stimulation for a representative animal ($p < 0.001$, uncorrected). Each scan

represents a ~7 minute acquisition collected within the same session. White triangles indicate the site of stimulation. Image numbers correspond to coronal slices shown in Figure 1B. (*B*) Average fMRI time series measured at the site of stimulation (LPFC) and ipsilateral thalamus illustrate the high degree of consistency in evoked responses over repeated trials. Time series come from the same scans shown in (A). (*C*) Activation maps in response to 40 Hz stimulation for each of the 11 animals reported in Figure 1 ($p < 0.001$, uncorrected). (*D*) Average fMRI time series measured at the ipsilateral LPFC and thalamus for each animal, illustrating the high degree of inter-subject reproducibility. Time series come from the same scans as shown in (C).

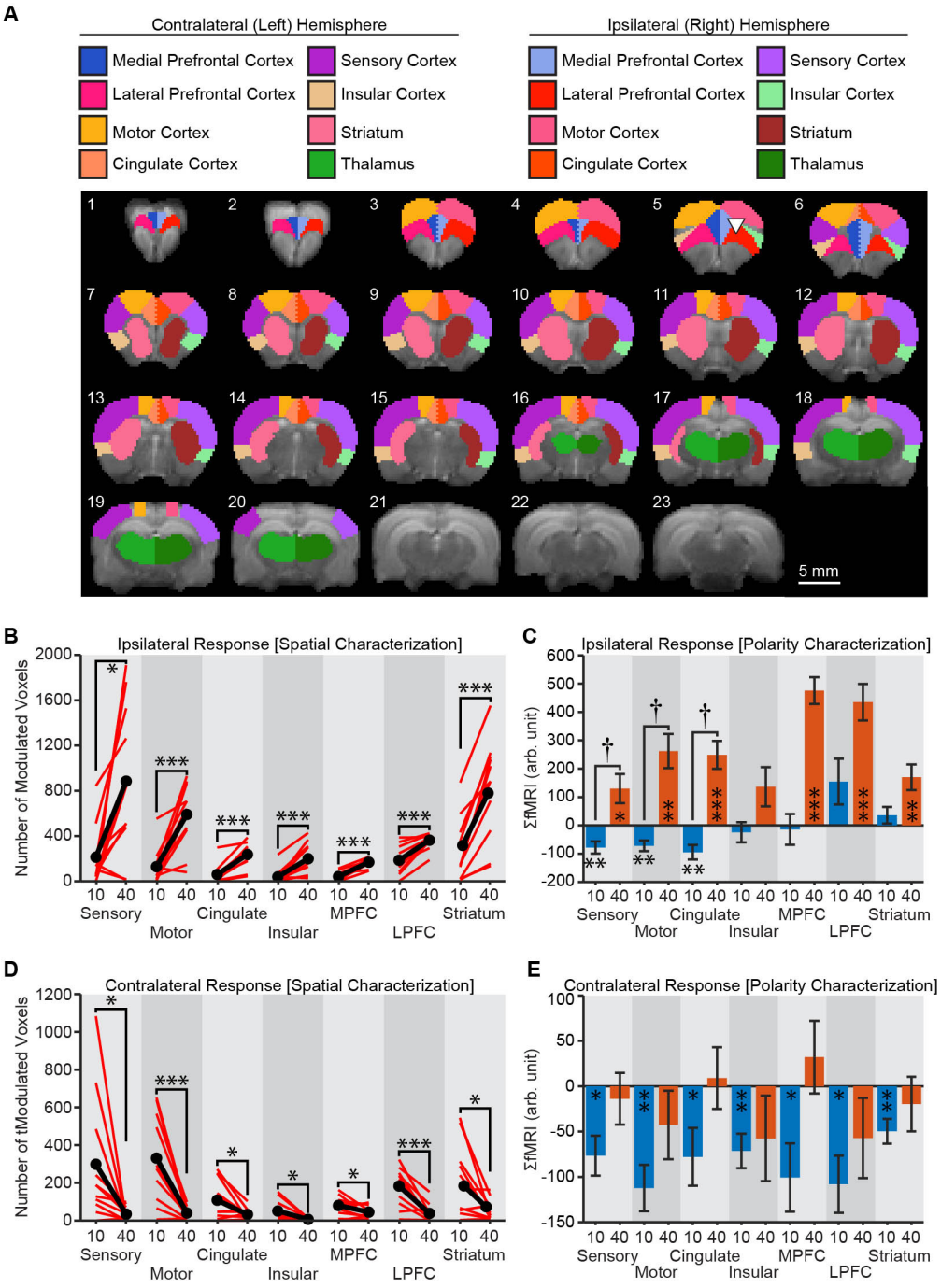

Figure S3. Quantitative, ROI-based characterization of fMRI responses evoked during thalamocortical stimulation; Related to Figure 1. (*A*) Brain-wide fMRI activations were segmented according to anatomical regions of interest (ROIs) for quantitative analysis of spatiotemporal properties. Segmented ROIs are overlaid as colored regions on the average structural MRI image. (*B,D*) Quantification of modulated voxels in ipsilateral (B) and contralateral (D) regions of interest during 10 and 40 Hz stimulation. Ipsilateral volume is significantly greater

during 40 Hz stimulation, while contralateral volume is significantly greater during 10 Hz stimulation (*$p < 0.05$, **$p < 0.005$, ***$p < 0.001$). Red lines indicate values from individual animals. Black lines represent the mean. (*C,E*) Quantification of ∑fMRI values in ipsilateral (C) and contralateral (E) regions of interest with significant differences from zero marked with asterisks. Three ipsilateral regions – sensory, motor, and cingulate cortex – switch from a significant negative response at 10 Hz to a significant positive response at 40 Hz (†). Contralateral ∑fMRI values are significantly negative during 10 Hz stimulation, but not significantly different from zero during 40 Hz stimulation. Values with error bars represent mean ± s.e.m.

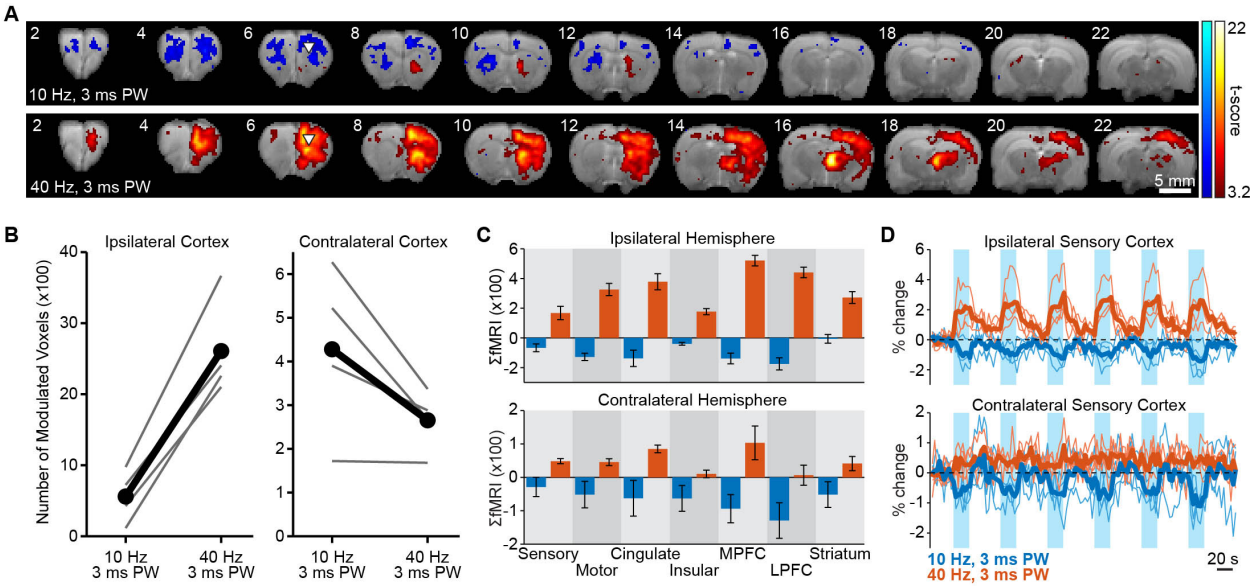

Figure S4. The frequency-dependent effects of thalamocortical projection stimulation are preserved when pulse width (PW) is held constant; Related to Figure 1. (*A*) Activation maps from a representative animal during 10 and 40 Hz thalamocortical stimulation in VLO using a constant pulse width of 3 ms ($p < 0.001$, uncorrected). White triangles on slice 6 indicate the approximate site of stimulation. Warm colors indicate positive t-scores, while cool colors indicate negative t-scores. Image numbers correspond to coronal slices shown in Figure 1B. (*B*) Quantification of total fMRI modulation volume in ipsilateral and contralateral cortex (N=4 animals). Thin gray lines correspond to individual animals. Black lines represent the mean. Values were summed over cortical ROIs. (*C*) Quantification of ∑fMRI values for ipsilateral ROIs. Error bars represent mean ± s.e.m. over animals. (*D*) Time series from the ipsilateral and contralateral somatosensory cortex. Thin lines indicate the response of individual animals. Thicker lines represent the mean.

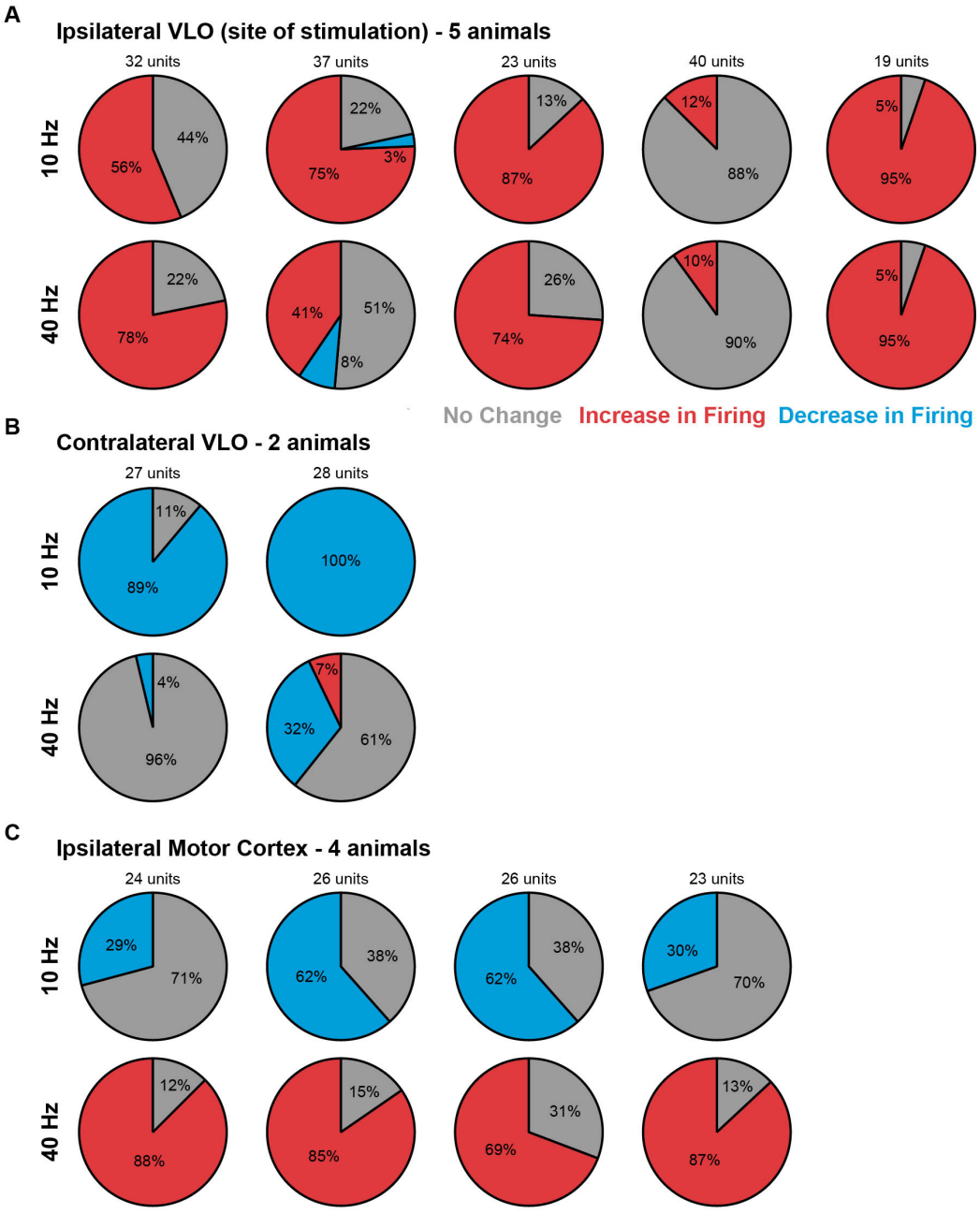

Figure S5. Animal-specific electrophysiology results reflect the frequency-dependent trends reported in the main text; Related to Figure 4. Each column represents a different animal used for single-unit recordings at the site of stimulation in VLO (*A*), in the contralateral VLO (*B*), or in the ipsilateral motor cortex (*C*).

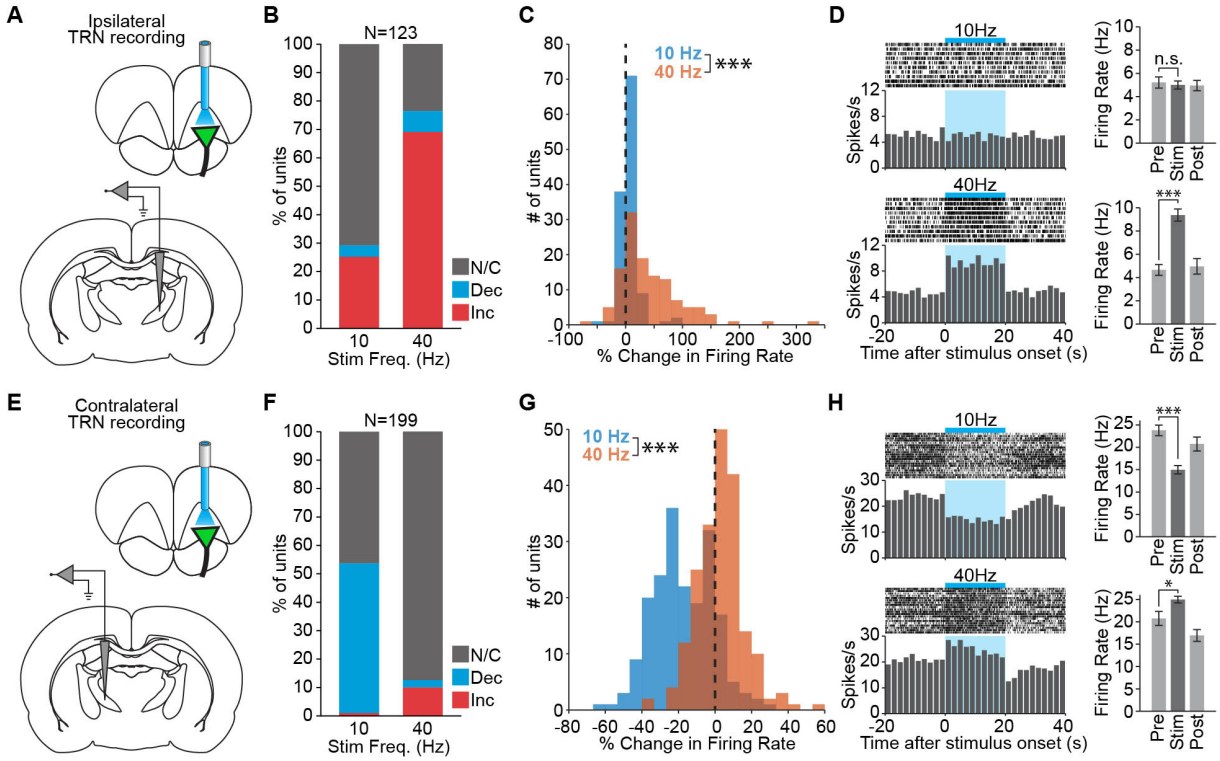

Figure S6. Stimulus-evoked activity in the thalamic reticular nucleus (TRN) is greater during 40 Hz thalamocortical stimulation than during 10 Hz stimulation; Related to Figure 5. (*A,E*) Schematic of single-unit recording locations in ipsilateral (A) and contralateral (E) TRN during thalamocortical stimulation in VLO. (*B*) Quantification of significant changes in firing rate in the ipsilateral TRN. More units exhibit a significant increase in firing rate during 40 Hz stimulation. INC: increase, DEC: decrease, N/C: no change. (*C*) Histograms of stimulus-evoked changes in firing rate within the ipsilateral TRN during 10 and 40 Hz stimulation ($p=5.3x10^{-12}$). (*D*) Peri-event time histograms from a representative unit in ipsilateral TRN that exhibits a significant increase in firing rate during 40 Hz stimulation ($p=1.6x10^{-4}$), but no change during 10 Hz stimulation ($p=0.39$; n.s. not significant). Error bars represent mean ± s.e.m. over trials. (*F*) Quantification of significant changes in firing rate in the contralateral TRN. Activity preferentially decreases during 10 Hz stimulation. (*G*) Histograms of stimulus-evoked changes in firing rate within the contralateral TRN during 10 and 40 Hz stimulation ($p=6.6x10^{-31}$). (*H*) Peri-event time histograms from a representative unit in contralateral TRN that exhibits a significant decrease in firing rate during 10 Hz stimulation ($p=7.7x10^{-8}$) but a significant increase in firing rate during 40 Hz stimulation ($p=0.020$).

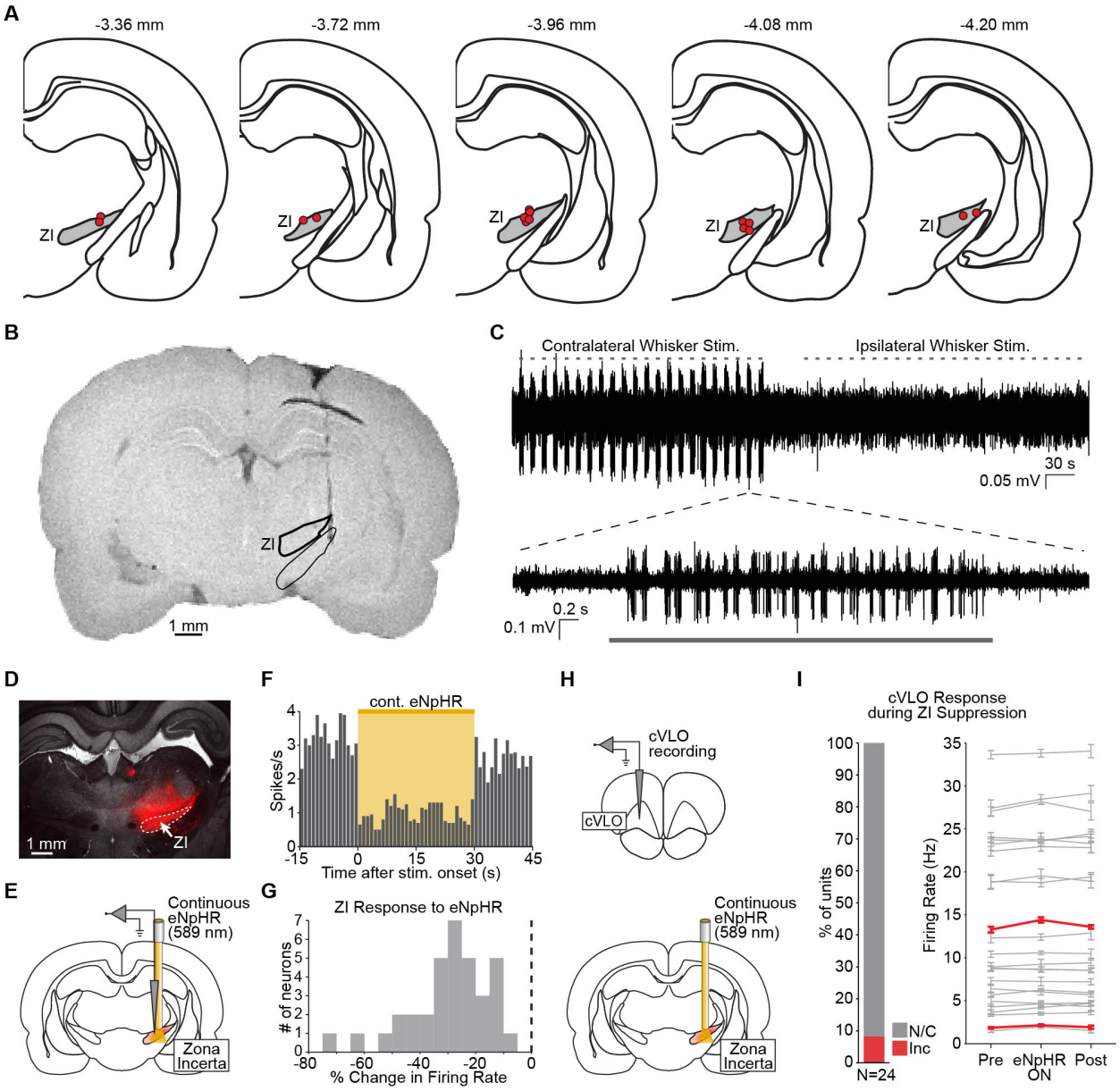

Figure S7. Methodological details of zona interta targeting and control; Related to Figures 6 and 7. (*A-C*) Stereotactic targeting is accurately localized to zona incerta (ZI). (*A*) To assess the accuracy of stereotactic targeting in zona incerta, bilateral implants were inserted to the target coordinate [-3.96 mm AP, ±2.75 mm ML, -7.20 mm DV] in a separate cohort of animals (N=9). The resulting implant locations were identified with MRI. Individual implants, represented in the schematics as red circles, were all located directly above or within the zona incerta [average location: -3.92 mm AP, ±2.79 mm ML, -7.21 mm DV]. (*B*) High-resolution *ex vivo* MRI scans confirmed the correct placement of the infusion cannula in zona incerta during lidocaine hydrochloride experiments. Region outlines for zona incerta and the below white matter tracts are

overlaid for clarity. Fast low angle shot (FLASH) MRI sequence parameters: 0.1x0.1x0.08 mm^3 spatial resolution, 280x280 matrix size, 12.9 ms TR, 4.9 ms TE, 170 slices, 30° flip angle. (*C*) Electrophysiology signal recorded at the target coordinate in ZI during eNpHR experiments (high-pass filtered, 300 Hz cutoff frequency, 4-pole Bessel filter). Neurons at the target coordinate are responsive to 4 s periods of contralateral, but not ipsilateral, whisker stimulation, consistent with known receptive field properties of zona incerta (Nicolelis et al., 1992). Bottom trace shows a zoomed-in version of one contralateral whisker stimulation trial. (*D*-*G*) Histological and functional confirmation of halorhodopsin expression in zona incerta. (*D*) mCherry expression in zona incerta confirms expression of eNpHR-mCherry. (*E*) Recordings were performed in zona incerta during continuous 589 nm light delivery there to confirm functional halorhodopsin expression. (*F*) Peri-event time histogram from a representative unit in zona incerta that exhibits a significant decrease in firing rate during eNpHR activation ($p=1.3x10^{-5}$). A significant decrease in firing rate was observed in all recorded units (N=35 units, 20 trials). (*G*) Histogram of eNpHR-driven changes in firing rate across all recorded units in zona incerta (N=35 units). The average change in firing rate was -30% ± 15% s.t.d. (*H*) Recordings were performed in contralateral VLO during continuous suppression of zona incerta to investigate any tonic influence of ZI over cortex. (*I*) The majority of units recorded in contralateral VLO (92%) exhibited no significant change when zona incerta was inhibited with halorhodopsin. 8% exhibited a significant increase in activity.